

Development of an acoustic process monitoring system for selective laser melting (SLM)

N. Eschner*, L. Weiser*, B. Häfner*, G. Lanza*

*wbk – Institut für Produktionstechnik, Karlsruher Institut für Technologie, 76131 Karlsruhe

1 Abstract

The current selective laser melting (SLM) process lacks both process quality and reproducibility. Recent research focuses on the integration of optical measuring technology, but acoustic sensors also seem promising. Initial results on acoustic methods show their suitability. The further processing of the data still shows difficulties, mostly due to the high sample rate. In this work a concept for an acoustic process monitoring system is developed and integrated into the process. First results show its capability to distinguish different process qualities.

For this purpose, various configurations for in-process integration of acoustic measurement techniques are discussed and evaluated. The most promising structure-borne sound concept is integrated and tested in a test bed. In a Design of Experiments for specific parameter selection, cubes with different process qualities are produced, and the acoustic signatures are evaluated. For a first prove of concepts a Neuronal Network is trained to classify three different laser classes. Therefore, different NN topologies were tested and the best-found solution had a precision of more than 90%.

2 Introduction/Motivation

Additive manufacturing (AM) enables a high level of functional integration, the capability of rapid prototyping, individualized products as well as economical production in small series. As a result, additive manufacturing processes are becoming increasingly important in many industries. The laser beam melting (LBM or more commonly known as SLM) is focused, since it is an established process in the area of prototype construction that stands at the threshold for the employment in large and small series production (Kief, Roschiwal & Schwarz 2015). The SLM process is a powder-bed-based process in which metal powder is melted layer by layer using a laser to form a solid body (Gebhardt 2016).

If material defects occur during the process, they lead to an undefined reduction in fatigue resistance and a shortened life of the components (Yadollahi & Shamsaei 2017). This means that components can only be used at highly stressed and safety-relevant points once complex end of line quality assurance has been implemented. Focusing serial production with this manufacturing technique an end of line quality assurance is much too expensive and has to be mitigated. . (Lanza et al. 2017)

To avoid costly end of line quality assurance, as well as guarantee the durability of the AM parts, a suitable process monitoring method that is integrated into the build process is advantageous. It is essential that the recorded data gets processed in a way that the information helps to ensure the required process quality. With an information about the actual process quality the built process can be stopped, or process parameters be changed to mitigate further defects.

Among the different kind of defects inner defects are of special interest. For porosity, some aircraft companies have defined a maximum diameter of 200µm to ensure the durability of AM parts. (Kiefel, Scius-Bertrand & Stöbel 2018) Other work has shown that the shape and the location in relation to the outer surface has a significant role on the fatigue resistance. (Reschetnik 2017) This makes it necessary to integrate process monitoring techniques that give quantitative information about shape, location and size of inner defects like pores.

This work will first investigate current existing techniques upon their capabilities before suggesting an acoustic measuring setup and presenting first results proving this concept.

3 State of the art

In this section a short review of SLM defect characteristics will be given and existing process monitoring techniques are discussed. Furthermore, the approaches to visualize the results of this monitoring techniques are introduced. This is followed by the discussion about systematically introduced defects in reference test bodies for evaluating the capabilities of process monitoring techniques. The last part of this section focuses on the discussion of relevant reference measurement techniques to evaluate location and shape of pores in AM parts.

3.1 Defects in SLM

There are different characteristic defects in SLM (Everton et al. 2016; Grasso & Colosimo 2017). Pores are of special interest since they are difficult to detect by end of line inspection and have a major influence on the fatigue behaviour (Leuders et al. 2013). To evaluate the influence it is important to know the shape and location of each pore (Reschetnik 2017), which strongly correlates with its formation mechanism.

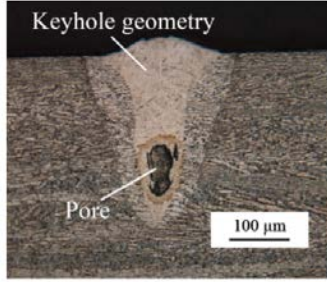
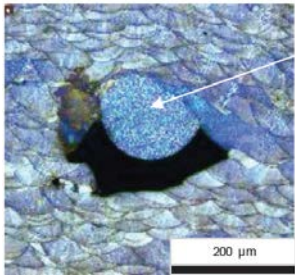
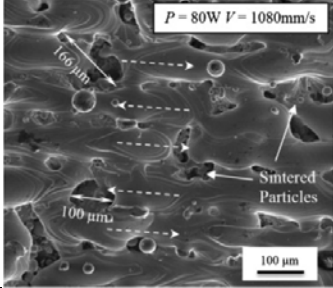
Too High Energy		Too Low Energy
Keyhole/Vaporization	Spatter	Unmolten powder
		
(Gong et al. 2014)	(Haeckel 2017)	(Gong et al. 2014)

Table 1: Pores may result from either bringing in too high or too low energy in the process zone (Gong et al. 2014)

When bringing in too high energy keyhole phenomena may occur, which result in subsurface pores. These kind of pores often have a spherical shape and indicate high concentrations of alloys with low vaporization temperature due the high temperature at the bottom of the melt pool, shown in Table 1 (Liu et al. 2016). Another phenomenon which is likely to occur from too high energy input is the generation of spatter which results from the recoil pressure spattering molten material (Khairallah et al. 2016). This molten material is likely to form a spherical shaped drop somewhere on the powder bed. Even though there are a few other phenomena resulting in powder bed contamination in the end this powder bed contamination cannot be melted completely and is likely to trap unmolten powder under it. (Haeckel 2017) The micrograph of such pore resulting from powder contamination is shown in Table 1-middle. Not only does spatter lead to insufficiently molten powder, if there is a too small overlap in scan strategies or insufficient laser power input, welding lines are only partly connected like shown in Table 1 on the right. (Gong et al. 2014; Thijs et al. 2010)

By tuning the process parameters, it is possible to mitigate pores resulting from too low or too high energy input. Despite this, process and melt pool instabilities from powder bed contamination or attenuation of the laser power from process gases, resulting in discontinuity energy input, can't be avoided completely. In total there are more than 50 process parameters influencing the SLM process which have to be considered. (Spears & Gold 2016; van Elsen 2007) Only few are correctly user controlled and they have only been partially researched. This shows the necessity of process monitoring or process integrated measurement techniques capable of detecting and quantifying pores.

3.2 Sensors for process monitoring

To detect process discontinuities which may result in pores, different in-situ process monitoring techniques exist. These are summarized in table 2. They can be divided in optical and acoustic monitoring techniques. Most of these methods are already known from laser welding. (Purtonen, Kalliosaari & Salminen 2014) There are first works also evaluating eddy current testing and backscatter computed tomography. These methods are up to date not yet implemented. (García-Martín, Gómez-Gil & Vázquez-Sánchez 2011)

First process monitoring techniques available in industrial application focus on the integration of optical measuring equipment in the beam path (Berumen et al. 2010; Everton et al. 2016). By integrating cameras and diodes/pyrometers into the optical path it is possible to quantify melt pool size, shape and radiation from the melt pool (Clijsters et al. 2014; Furumoto et al. 2013). With this information it is possible to realize a closed-loop control to reduce the occurrence of too high energy input and thereby the number of produced pores can be reduced. Further work also showed a correlation of position data of the laser with data from the melt pool monitoring, resulting in maps for each layer which help the operator to identify process variation, but cannot give a quantitative feedback about occurred defects and part quality. (Grasso & Colosimo 2017)

A more complex on-axial measurement technique is the optical coherence tomography, where a second laser system is integrated in the beam path (Neef et al. 2014). It might even be upgraded with a separate galvanometer-system scanning the melt pool (Kanko, Sibley & Fraser 2016). This technique achieves a new level of information, making it possible to evaluate further melt pool properties like keyhole depth and the geometrical profile of the melt pool.

The integration of Off-Axial sensors have the scope to monitor powder bed properties or scan path/scan surface (Grasso & Colosimo 2017). For observing the scan path or scan surface, pyrometers (Doubenskaia, Pavlov & Chivel 2010; Islam et al. 2013) or IR Cameras (Krauss, Eschey & Zaeh 2012) can be integrated. For observing the powder bed, cameras (Zur Jacobsmühlen et al. 2015) or laser line scanners (Haeckel 2017) can be used. For scientific purposes and to understand the process as well as melt pool dynamics, a high speed camera close to the process zone was integrated. (Ly et al. 2017)

Besides the above discussed optical monitoring methods mentioned, there are novel works elaborating further non-destructive testing techniques. Existing works an all four different kinds of non-destructive testing methods are summarized in Table 2.

There are first works on Eddy Current Testing integrated in the process, which right now is related with a high effort scanning the surface and thereby slows down the process. (García-Martín, Gómez-Gil & Vázquez-Sánchez 2011)

Rieder integrated an ultrasonic transducer under the build platform which can detect porosity by pulse reflection method. In this case an ultrasonic wave is generated by the transducer and the reflected wave from the backwall or defects is analysed. (Rieder et al. 2016) For this active acoustic approach an acoustic signal must be generated. The spatially resolved acoustics emissions approach, introduced by (Smith et al. 2016) works in a similar way. Surface acoustic waves are generated with a laser and the propagation is evaluated by measuring the surface acoustic wave at a second point. (Ye et al. 2018) introduced a passive acoustic approach measuring the airborne acoustic signature. Due to plasma generation it is possible to evaluate process discontinuity and detect overheating and balling.

Beside of these monitoring techniques first concepts are available for integrating an X-Ray into the process. This approach promises a high degree of information about inner defect. (Shedlock, Edwards & Toh 2011)

Optical		Eddy Current	Acoustic		CT
Off-Axis	On-Axis		Active	Passive	

High-speed camera (Ly et al. 2017)	Camera + diode (Berumen et al. 2010; Clijsters et al. 2014; Furumoto et al. 2013)	(García-Martín, Gómez-Gil & Vázquez-Sánchez 2011)	Ultra sound emissions-reflexion (Rieder et al. 2016)	Air borne acoustic emissions (Ye et al. 2018; Shevchik et al. 2018)	X-ray backscatter (Shedlock, Edwards & Toh 2011)
IR camera (Krauss, Eschey & Zaeh 2012)			Spatially resolved acoustic emission (Hirsch et al. 2017; Smith et al. 2016)		
Pyrometer (+Camera) (Islam et al. 2013; Doubenskaia, Pavlov & Chivel 2010)	High-speed Camera (Lott et al. 2011)				
Camera (Pulverbett) (Zur Jacobsmühlen et al. 2015)	OCT (Neef et al. 2014; Kanko, Sibley & Fraser 2016)				
Laser line scanner (Haeckel 2017)					

Table 2: Literature overview on process monitoring systems for the SLM process

3.3 Data evaluation of process monitoring

The monitoring techniques described above are in the development phase and have different scopes of application. Not all of them will be used in productive SLM systems in the future. As soon as a technology comes out of the development phase, during which process engineers operate the machine, it is necessary to get intuitive and clear feedback about the process quality. For this purpose, visualization techniques are used to show deviations in a 2D or 3D image like shown in ((Krauss 2016)). Figure 1 shows areas marked in red, in which high IR radiation from the melt pool is observed. This is an indicator for too high energy input and therefore likely to cause defects. (Krauss 2016) This kind of visualizations require interpretation by an expert and may be improved by automated pattern recognition algorithms. (Zenzinger et al. 2014)

Besides visualizing process deviations, a classification directly from raw signals is possible. A classification approach using machine learning algorithms for five classes was shown by (Ye et al. 2018), who were able to distinguish balling (a), light balling (b), good process (c), light overheating (d) and overheating (e) like shown in figure 2 by using the air borne acoustic raw signal. This classification of defects in combination with giving an indicator of the severity makes it easier for machine operators or automatized control systems to take the right actions or even precautions to prevent further defects in the process.

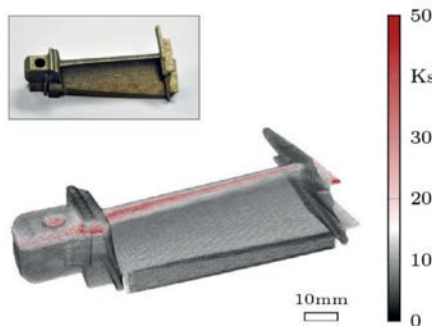


Figure 1: Data evaluation of a process monitoring technique (Krauss 2016)

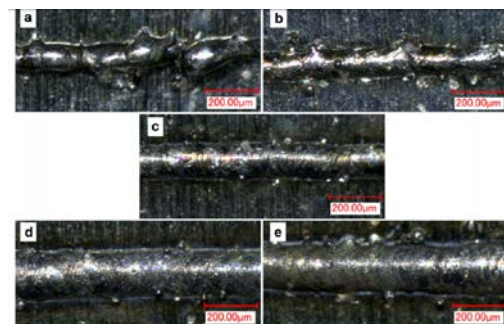


Figure 2: Distinguishing of classes: balling (a), light balling (b), good process (c), light overheating (d) and overheating (e) (Ye et al. 2018)

3.4 Reference bodies

The systematic introduction of defects or process characteristics in reference bodies is a common approach to evaluate the performance of process monitoring techniques. The most simple way to do this, is the creation of

single welding tracks like (Ye et al. 2018). This is especially advantageous since no complex measurement technique is needed to evaluate the properties of the welding tracks.

More complex three dimensional reference bodies are used by (Rieder et al. 2016) or (Toepfel et al. 2016). To systematically introduce defects different parameters are used. They range from parameters correlating directly with the energy input (layer thickness, laser power, scan speed, hatching distance) to inert gas flow or powder bed contamination. Table 3 gives an overview over considered defects and the used process parameters. Beside of these used process parameters there are much more process parameters which affect process quality and are not yet used for evaluating process monitoring techniques since they are difficult to vary. (Krauss 2016; Spears & Gold 2016)

Research approach	Considered parameter	Changed process parameter
(Rieder et al. 2016)	Density	Laser power
(Toepfel et al. 2016)	Pores/density	Laser power, hatch distance, geometry, scanner time delay
(Ye et al. 2018)	Balling/overheating	Laser power
(Haeckel 2017)	Pores	Powder bed contamination
(Zenzinger et al. 2014)	Pores	Inert gas Flow
(Krauss, Eschey & Zaeh 2012)	Pore	Laser Power

Table 3: Overview of considered defects and varied process parameters

3.5 Reference measurement technique

If reference bodies are produced it is essential for qualifying the measurement technique to have a reference to measure the introduced defects. To get information about the inner defects like pores different measurement techniques are suitable, each having its own advantages. In total, three different types are worth to be considered: Archimedes density measurement, micrographs and computer tomography (CT) (Spierings, Schneider & Eggenberger 2011)

Density measurements according to Archimedes have the lowest degree of information since it only gives a number of the overall density but no information about the location or particular shape of pores. Beside of this, the reproducibility and standard deviation of Archimedes measurement is the best of the three mentioned measurement techniques. (Spierings, Schneider & Eggenberger 2011)

Micrographs give the opportunity to evaluate the shape of pores and the location in the cross-section. This gives more information about pore properties than Archimedes measurement. By using microscopes, the usable resolution of this approach goes down to a few micrometres. Unfortunately the process of making micrographs with grinding, polishing and the parameters for taking pictures to evaluate the pores are hard to reproduce. (Spierings, Schneider & Eggenberger 2011)

The highest amount of data about the reference body can be generated by using a CT. With CT it is possible to evaluate size and shape of the pores according to BDG P202 (BDG 2010) over the whole volume of the test body. Major drawback of this technique is its measurement uncertainty and its undefined limit for small pores. Depending on the used parameter for the image acquisition the resolution of the CT image changes. (Schild et al. 2018)

4 Methodical approach

In this section the overall approach for developing an acoustic monitoring system will be explained. Therefore first of all the reasons for investigating an acoustic measurement setup will be explained before its integration into a test bench will be shown. In section 4.2 the design of the chosen reference bodies and the chosen defect mechanisms are introduced. Section 4.3 focuses on the data processing of the acoustic signal and the correlation of the features generated from the reference measurement.

4.1 Sensor and test setup

4.1.1 Selection of measurement technique

Figure 3 summarizes the capabilities of the different non-destructive testing (NDT) methods in general and compares their abilities in resolution and defect position (inside or surface) in a qualitative way. Since eddy current testing is only capable of detecting defects close to surface all techniques above the red line can detect defects inside a volume. The ones below the red line can detect surface or close to surface defects.

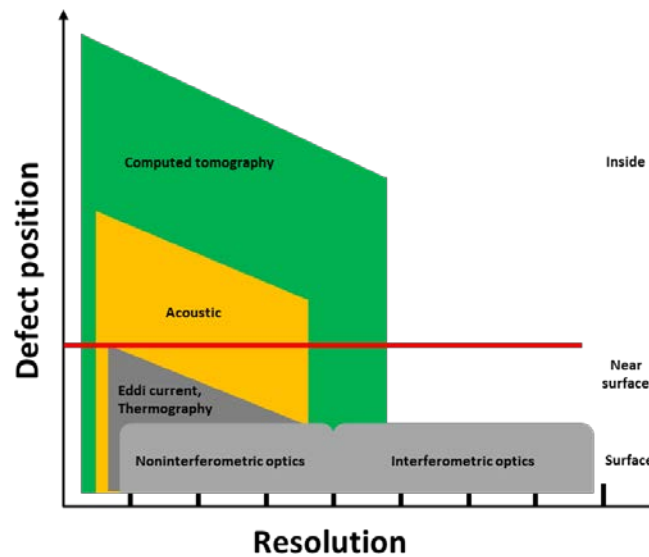


Figure 3: Comparison of NDT methods in resolution and defect positioning according to Gevatter & Grünhaupt 2006)

Section 3.1 showed that the formation mechanism of SLM characteristic pores only partly understood and there are works indicating the pore formation taking place without being visible at the surface (Calta et al. 2018). Nevertheless, pores are volume defects which makes it necessary to have a closer look on the testing methods which are in general capable of evaluating defects within the volume.

X-ray backscatter tomography, which is a special method of the computed tomography (CT), is part of further research and not yet integrated in the process. The process integration of CT was already shown for FDM and is also plausible for SLM. Regarding the high integration effort and investment cost, this is likely to be limited for research and special applications. Since the integration of acoustic sensors is much less complex (as shown in (Rieder et al. 2016; Ye et al. 2018)), it is promising to have a closer look on this kind of measuring principle.

4.1.2 Integration concepts of acoustic measurement systems

The generation and detection of acoustic signals in general can be performed by three different kind of actors/sensors: piezo, electromagnetic transducer (EMAT) or by the laser itself. Furthermore, acoustic waves can be air borne or structure born. This work will focus on structure born noise due to its expected higher degree of information.

With regard to the integration of the actor and the sensors, there are two general placements, which are schematically sketched in figure 5 as variants A and B. In variant B, the probe is mounted in the available space between the construction platform and the substrate plate. Such a construction has already been implemented and tested (Rieder et al. 2016). Variant A provides space for the sensor to be positioned above the workpiece or

integration into the beam. The installation space above the workpiece is limited by the fact that the beam path of the laser must not be disturbed. Nevertheless, this variant offers advantages in terms of component coverage.

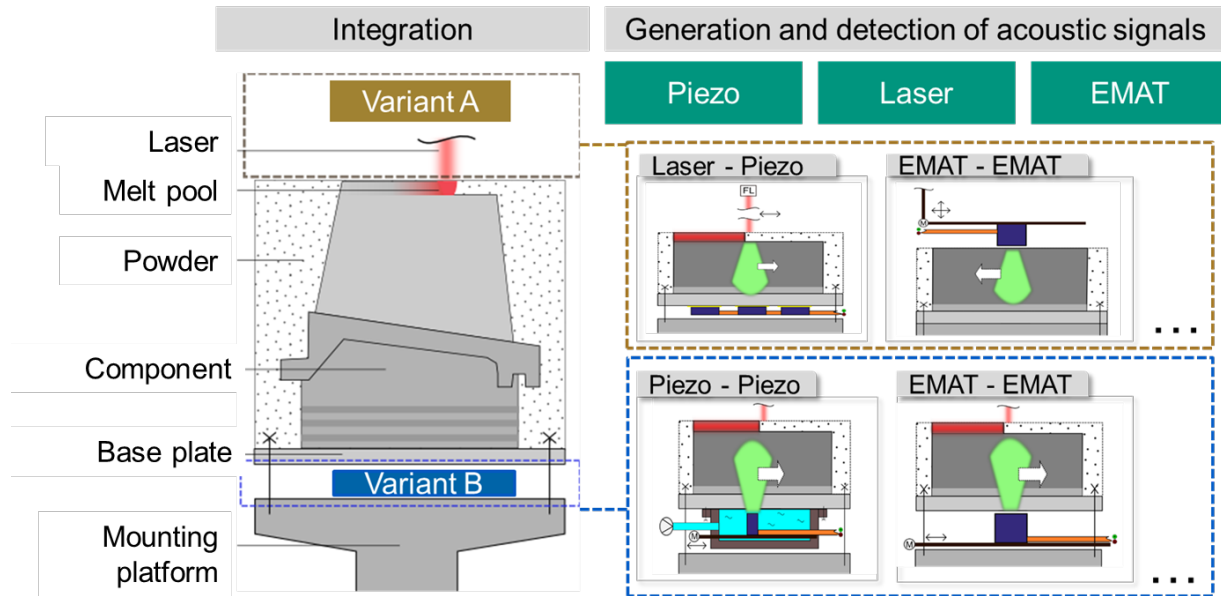


Figure 4: Integration and signal generation/detection options for SLM process monitoring

With these options to integrate sensors and the three sensor options to generate/detect acoustic signals, 18 different options for acoustic testing in SLM can be generated. 9 concepts are plausible and worth of further discussion which can be found in (Eschner et al. 2017) and will be only summarized here.

- In general, the integration above in volume A of a piezo electric or EMAT makes it necessary to implement a mechanism to move the transducer for signal detection over the process zone in order to not interact with the laser beam. Such mechanisms are complex, susceptible to failure and slow down the overall process time.
- When the laser induces energy, acoustic waves are generated which can be measured and evaluated like ((Ye et al. 2018)) has shown for air-borne acoustic emissions.
- It is likely to interact with ferromagnetic material and EMATs which lead to a disturbance of the powder bed.
- Low frequency ultrasonic transducers have limited performance in resolution, while high frequency ultrasonic transducers have limited access to the whole volume since the waves are damped excessively
- For the integration in variant A attention should be spent to the existing temperatures and the platform heating. Nevertheless, it was shown, that the integration at this position is possible.

To have an optimal solution regarding process time, expected information content and minimizing integration effort of the nine plausible concept one was favoured. The favoured concept is shown in figure 6 and will be explained in the following.

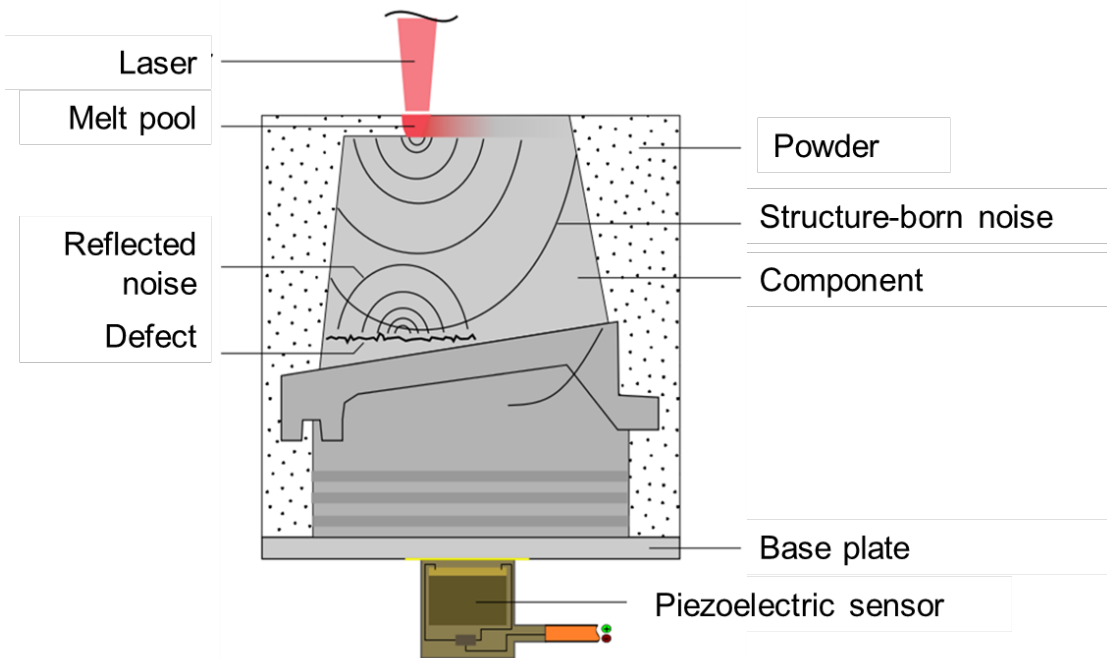


Figure 5: Monitoring concept for SLM using structure-borne acoustic emissions

In this concept, the acoustic waves are generated by the SLM process itself from plasma and other process dynamics. The generated waves propagate through the build object and are recorded by a piezoelectric transducer. If a defect, like a crack prevents the propagation recorded signals change. Furthermore, the process stability itself can be judged, since process inhomogeneity produces inhomogeneous signals. This concept is favoured since it monitors the building process and thereby promises the highest degree of information, while not slowing down the process. (Eschner et al. 2017)

4.1.3 Integration of an acoustic measurement system in a reference SLM process

In order to investigate the capabilities of the process monitoring technology, reference bodies are printed as shown in section 3.4 and systematic errors are introduced into them. For this purpose, it is necessary to have a process environment which gives the flexibility to vary process parameters freely and integrate the sensor. A test setup imitating the SLM process was designed, giving flexibility for the relevant process parameters and sensor integration.

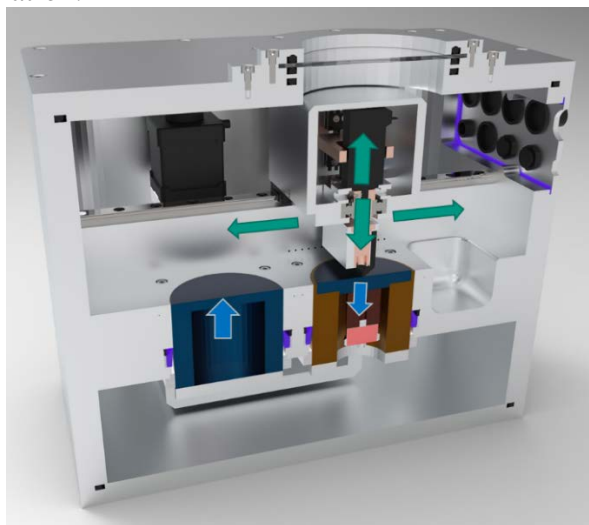


Figure 6: Sectional view of SLM build chamber in test setup



Figure 7: Complete view of test setup

Figure 6 shows a cross sectional view of the process chamber which is the central unit of the test setup. The powder application mechanism is a simple wiper mechanism to reduce overall complexity. There is one cylinder used as a powder reservoir. The wiper moves from left to right and applies the powder from the powder reservoir onto the build platform. The build platform moves down after a layer is exposed. Under the build platform an acoustic sensor by *QASS* is integrated. All axes are moved with stepper motors in micro stepping mode. Right next to the build platform, outlet and inlets for the inert gas flow are integrated. The outlets and inlets are easily replaced to influence the inert gas flow. The whole system is sealed against the environment to avoid oxygen contamination and to realize positive or negative pressure.

The process chamber is integrated in a machine frame made from standard profiles which connect all the different components (Figure 7). Since an acoustic sensor is used, some effort was spent for acoustic decoupling of peripheral equipment like computer or optical system with the scan head.

The laser system consists of a 250W IPG laser and a Cambridge Technology SMC scanner card. The XML API provided by Cambridge Technology offers a flexible adaption of process parameters. A python script generates the code needed for every layer of the test cubes. The cubes are then placed in a 3x3 matrix on the substrate plate. Every cube is printed with its own set of parameters. More complex objects are generated via a CAD/CAM chain consisting of a slicer software (*Slic3r* with a custom configuration suitable for SLM) and a python script converting the generated G-code into the according xml code. The printing parameters are also freely variable. A main *LabVIEW* application controls the stepper motors, the inert gas system, all sensors as well as the *QASS* ultrasonic measurement device. The data is recorded with a frequency of 4 MHz. The inert gas system is designed to have the ability to vary process parameters like flow rate and oxygen content. For this purpose, the system is equipped with an oxygen-, a temperature- and a flowrate sensor.

To get information about the actual position of the laser beam spot and to synchronize this information with the acoustic signal, a FPGA for interpreting the XY2-100 protocol (protocol for communication between scanner card and galvanometer scanner) of the galvanometer system was realized. With this system it is possible to assign a position to its corresponding acoustic signal during the build job.

4.2 Evaluation of the acoustic measuring system with reference bodies

To evaluate the acoustic measuring system in a first approach, reference bodies are printed with varying part quality. As shown in section 3.4 there are different ways for producing reference bodies. One of the easiest ways is to vary process parameters like laser power (P_{laser}), layer thickness (d_{layer}), scan speed (v_{scan}) or hatching distance ($d_{hatching}$). These four parameters directly correlate with the energy density which can be calculated as following:

$$E = \frac{P_{laser}}{v_{scan} * d_{layer} * d_{hatching}} \quad \text{(Formula 1)}$$

Previous work by (Cherry et al. 2015) (see Figure 8) and (Gong et al. 2014) (see Figure 9) have shown that the energy density within the process is correlated directly to the part quality, which was measured in these cases on porosity. There is an optimal interval, in which the process produces good results. Above and below the interval, quality drops rapidly (Gong et al. 2014; Cherry et al. 2015). Based on this knowledge, the varied process parameter to influence part quality regarding pores will be the energy density used in the process.

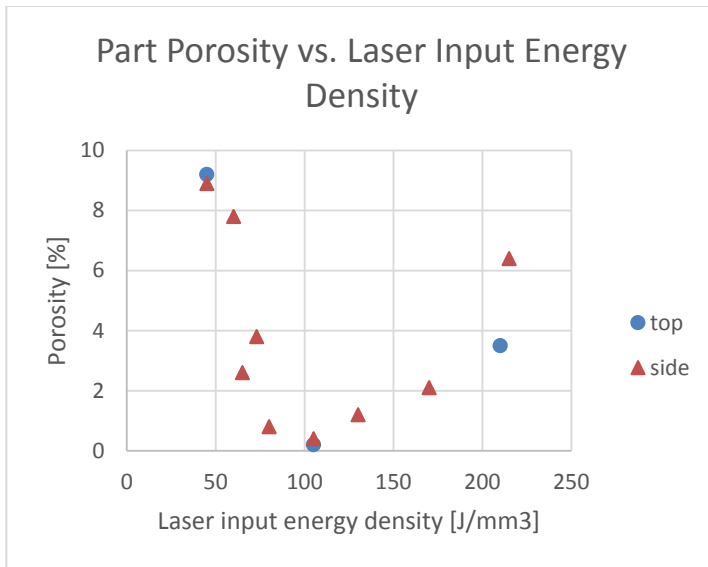


Figure 8: Relation between part porosity and energy density in (Cherry et al. 2015)

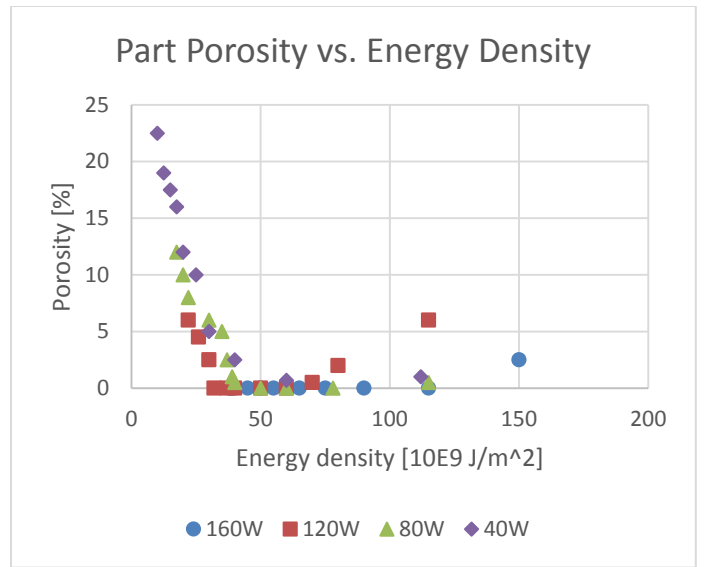


Figure 9: Relation between part porosity and energy density in (Gong et al. 2014)

To evaluate the capabilities of the acoustic monitoring technique, this correlation of energy density and part quality/porosity is used. Therefore, to obtain a wide range of energy inputs, a Design of Experiments (DOE) was conducted with the four parameters influencing the energy input. Since only four parameters are varied, a full factorial test plan is used. Each parameter range has a minimal value, a centre point and a maximal value.

The given formula for energy input (Formula 1) is a hyperbola, which means a true centre point of the min-max interval results in an unevenly distributed energy input throughout the test objects. To counter this effect, the centre value of the scan speed was set to a third of the interval range. The parameters were set as stated in Table 4:

Parameter	Minimal value	Centre value	Maximal value
Laser power	150 W	200 W	250 W
Scan speed	200 mm/s	400 mm/s	1000 mm/s
Layer thickness	0.02 mm	0.03 mm	0.04 mm
Hatching distance	0.03 mm	0.04 mm	0.05 mm

Table 4: Parameter set for Design of Experiments

The resulting 81 parameter sets are printed in the designed test setup as cubes with an edge length of 0.5 mm. The material used is 316L stainless steel. Each build job contains 9 different reference bodies as shown in Figure 10. Since a 3x3 matrix is printed on the substrate plate, the scan speed is varied in the y direction, the laser power in x direction (compare Figure 10). The other two parameters, layer thickness and hatching distance, are varied in between the different substrate plates. This results in a total of 81 test cubes on 9 substrate plates. To ensure an even distribution over all energy input levels, the energy input over the parameters as well as the number of the according substrate plate can be plotted (Figure 11)

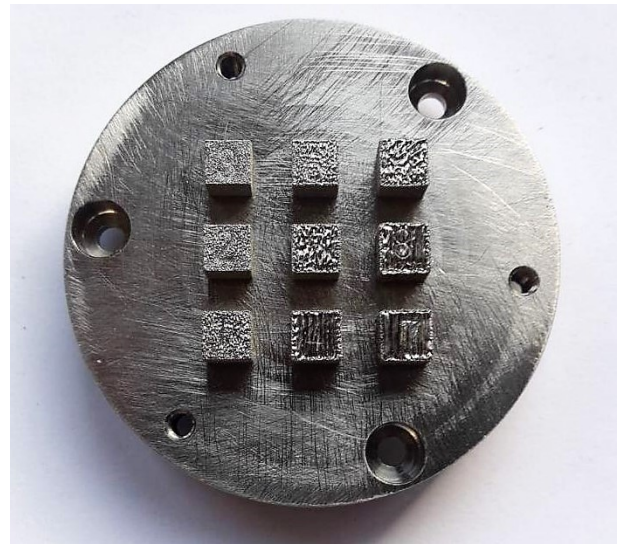
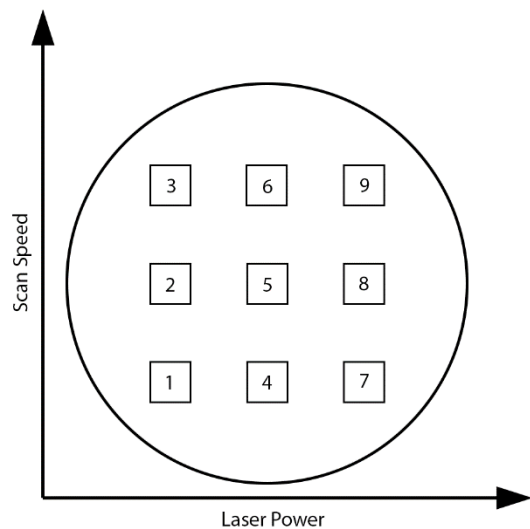


Figure 10: Substrate plate with 3x3 cube matrix and varied print parameters

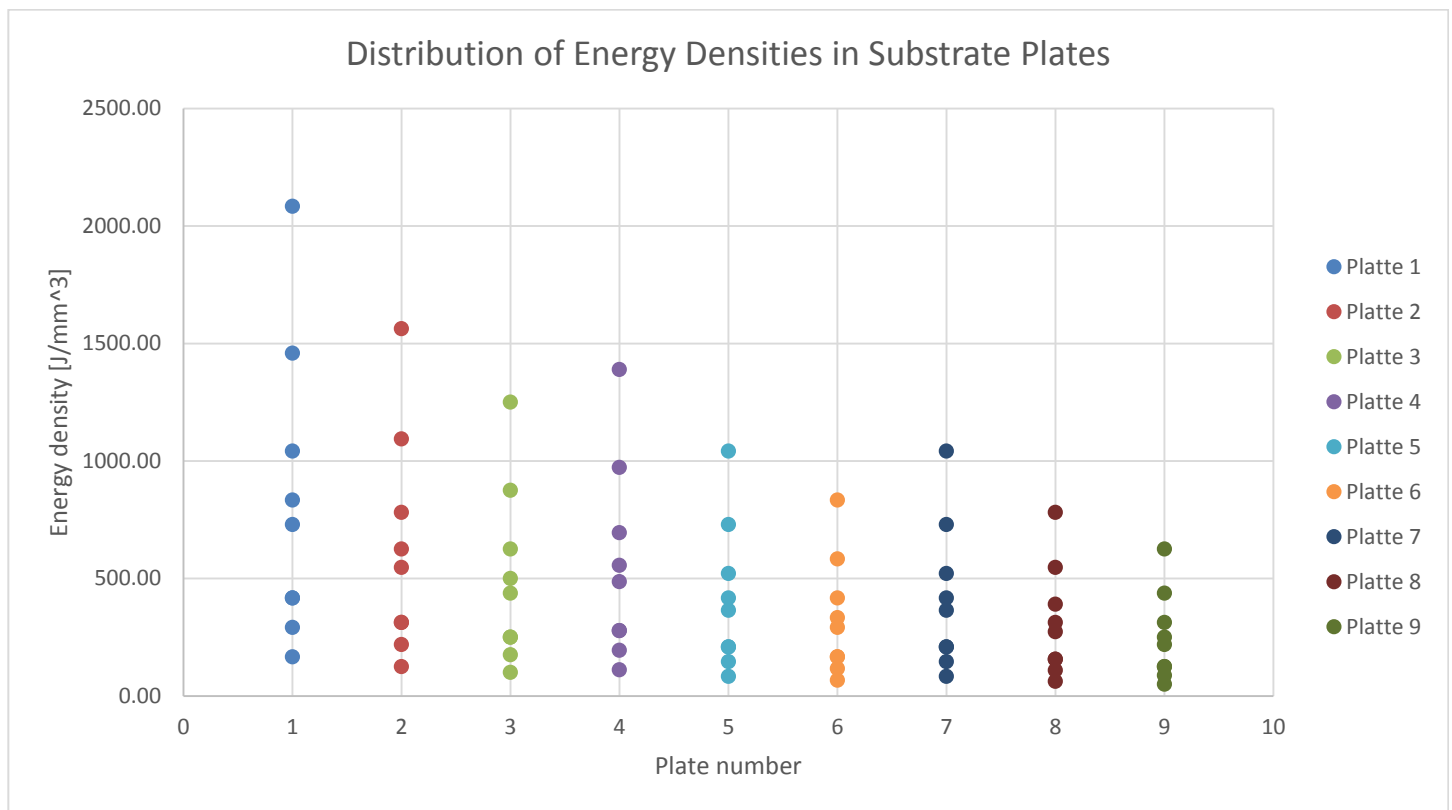


Figure 11: Energy density distribution over all substrate plates

Several tests conducted before setting up the test plan showed a rough estimate of the expected process window. An energy input between 500 and 1000 J/mm^3 seems to be optimal. For testing purposes, it is mandatory to achieve values below and under that interval, thus provoking process states with too high energy (resulting in keyhole mode / overheating) and states with too low energy (pores, partial melting of powder).

4.3 Correlating acoustic signals with reference measurements

The main objective of the utilised process monitoring technique is not to detect the variance between different processes, but rather to carry out an analysis of the component quality (with the associated defects) at coordinate level. The goal is to automatically determine the type of defect as well as the spatial extent and location in the component. Selected process parameters are to be validated automatically by a machine learning technique. If it is necessary to adjust parameters due to the current process situation, the system should propose a suitable parameter set.

To evaluate the printed test cubes, two methods will be used: computer tomography and Archimedes. The results of the reference measuring, the acoustic signal of the process (with extracted features) and the printing parameters are then compiled into datasets. These are then used to train an artificial neural network (ANN), which will be realized in Python's *sklearn* package and *Google TensorFlow*. To handle the great amount of data, most calculations will be done with GPU support (*Nvidia CUDA*).

For first analysis classification is used to determine the type of the main defect (overheating, balling, pores), whereas in future work regression will be used to get quantitative features like density value. The complete dataset is randomly split into training (70%) and test data (30%) to test repeatability of the training (each training is repeated five times and the according mean and standard deviation is calculated). To evaluate the model performance regarding a classification over the whole dataset, a five-time cross-validation is performed with an according 80/20-split of the data.

The raw input signal of the sensor is decoded from its binary and proprietary data format of the manufacturer into a *Pandas dataframe* which is stored with *zlib* compression as a *HDF5* file on disk. The timeseries is then fast fourier transformed (FFT) using a window of 0.005 seconds. As windowing function, the hanning window is used. To reduce background noise, a frequency mask of the background signal is subtracted from the resulting FFT (see Figure 13 and Figure 14). The result is a spectrogram for each layer like shown in Figure 12.

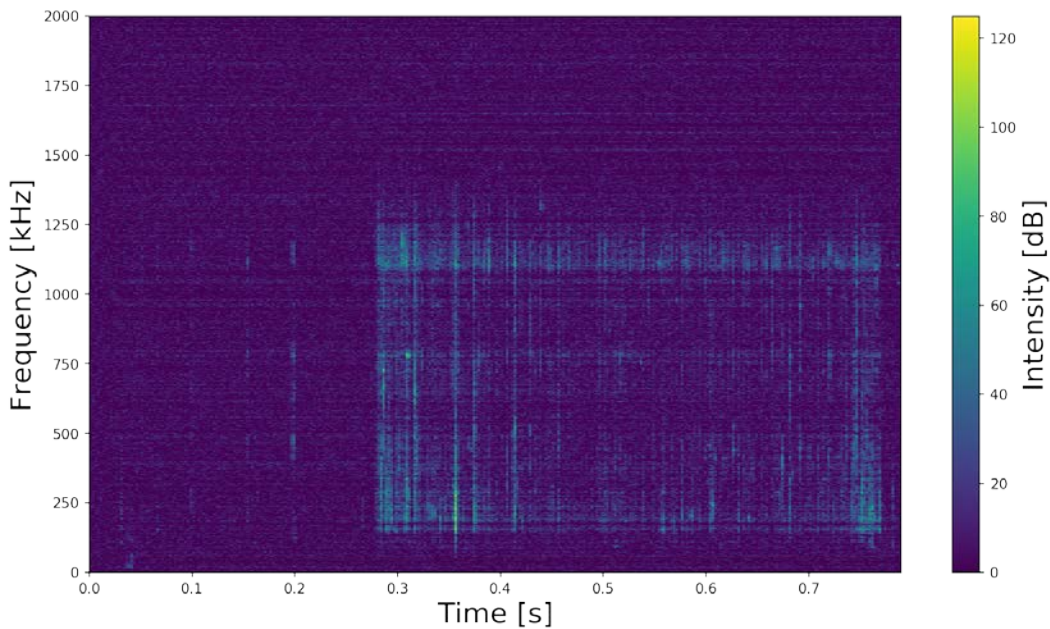


Figure 12: Spectrogram of measured signal of one layer (filtered)

To feed the FFT of each layer into the artificial neural network, the data must be flattened since they are stored as an array (Formula 2). The additional features can be added in the future to the input vector. The vector resulting directly from the spectrogram contains 12 million values, meaning one value for each pixel. To reduce

this amount, a bottleneck approach is used. The number of neurons in a hidden layer is set between five and a hundred. Performance of different topology will be tested.

$$\begin{bmatrix} x_{n=1}^{t=1} & \dots & x_{n=1}^{t=t_{max}} \\ \vdots & \ddots & \vdots \\ x_{n=n_{max}}^{t=1} & \dots & x_{n=n_{max}}^{t=t_{max}} \end{bmatrix} \xrightarrow{\text{flatten}} [x_{n=1}^{t=1} \dots x_{n=n_{max}}^{t=1} \dots x_{n=1}^{t=t_{max}} \dots x_{n=n_{max}}^{t=t_{max}}] = x_m \quad (\text{Formula 2})$$

The output vector can contain different types of output classes like scan speed, laser power, energy density, defect type (pore volume, pore shape, number of pores, ...) etc. from which an array of outputs can be created (Formula 3).

$$\{\text{list of output classes}\} \xrightarrow{\text{output selection}} [y_{m=1} \dots y_{m=m_{max}}] \quad (\text{Formula 3})$$

5 Results

This section will show first results of the above described methodical approach in detail. The results contain the analysis of 18 cubes build in two build jobs. Each cube has 120 usable layers (the first five layers were discarded due to double exposure), which leads to a total dataset of 2160 individual datasets. To gain first experiences with artificial intelligence (AI) data analysis, only the given laser power from the output vector was used. So, no features from the reference measurement technique is used for first exemplary evaluations of acoustic signals of the process. The analysis of all 81 cubes with the use of a reference measurement technique will take place in the future.

5.1 Capturing raw process data

For data processing, it is crucial to obtain a clear, noise free signal with a sufficient amplitude. First tests with a ceramic coupling between the sensor and the substrate plate showed a high dampening of the process sound. Therefore, the resulting measurements had to be discarded. After removing the ceramic coupling and adding glycerol as a coupling agent, the signal was much stronger. As a drawback, the background noise of the test setup (stepper motors, vibrations of the inert gas pump) were present and reduced the usable information within the signal. Using a difference mask (see Figure 13 and Figure 14) showed very good results in reducing noise from the test setup. The printing process of each layer was recorded by the *QASS* measurement system. The resulting time series was then transformed via FFT to the frequency domain. The process has an effective frequency range up to 1.3 MHz.

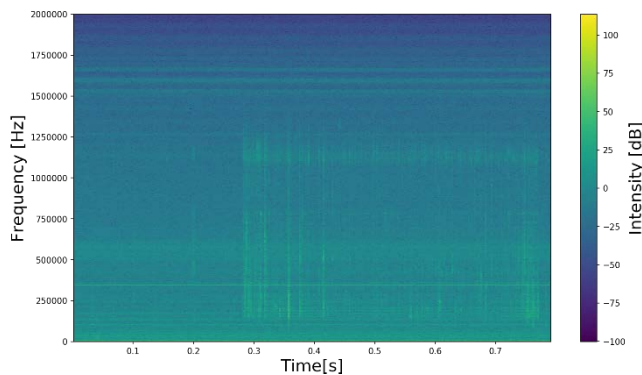


Figure 13: Raw measuring signal without applied filter

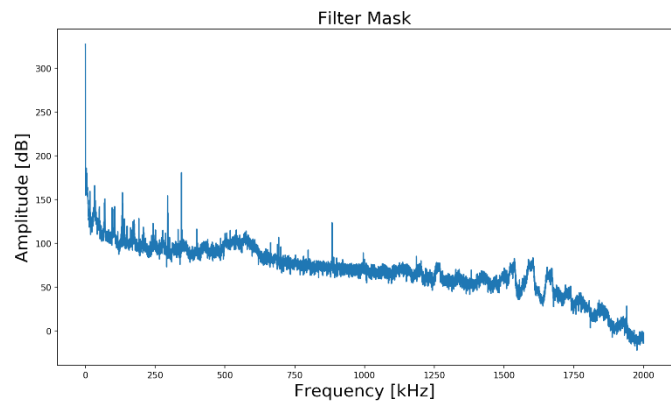


Figure 14: Difference mask to reduce noise from test setup

5.2 Data preprocessing

Each measurement is decoded and processed and stored along with its parameter set on disk. One substrate plate creates roughly 100 gigabytes of data. Every layer is then assigned with an output class: for the first test, the used laser power. For feeding the data into an artificial neural network, every dataset must contain an equal number of samples. To achieve this, the machine noise is appended at the end to fill to the desired length. During pre-processing, a dataset with input and output vectors is created and stored separately on disk to reduce processor (CPU) time for repeated use. The dataset is then randomised and split into 70% training data und 30% test data.

5.3 Artificial Intelligence

Utilizing *sklearn*'s `MLPClassifier`¹, a multi-layer perceptron is used to make a first attempt on classification. First results show a better performance of a stochastic gradient descent solver over the *ADAM* solver. As activation function, ReLu is used. Tanh was tested but produced worse results than ReLu.

¹ Scikitlearn: A python package which has a lot of built in ~~ML~~ and data processing functionality

Precision defines the number of true positive classifications in regard to all positive classifications (“What proportion of positive identifications was actually correct?”²), whereas recall is calculated by comparing the true negative classifications to all real positives (“What proportion of actual positives was identified correctly?”³). The F1-Score combines precision and recall via (Formula 4):

$$F1 = \frac{2 * (precision * recall)}{precision + recall} \quad \text{(Formula 4)}$$

To check the repeatability of training the artificial neural network, the network was trained and tested five times on the same split of training and test data. The mean and standard deviation of precision, recall and F1-score are shown in Figure 15 to Figure 20.

When regarding precision, recall and f1-score, one can notice that there is an interval of neurons in which the classification results are optimal. Above and below that interval the classification score drops rapidly. Furthermore, it can be seen that the addition of multiple hidden layers does not provide a increase regarding the reachable classification score. In contrary, when regarding the standard deviation it is noticeable that the standard deviation rises with the addition of more layers. This means that the training itself lacks repeatability and therefore gets more stochastic.

² From: <https://developers.google.com/machine-learning/crash-course/classification/precision-and-recall> [22.08.2018]

³ From: <https://developers.google.com/machine-learning/crash-course/classification/precision-and-recall> [22.08.2018]

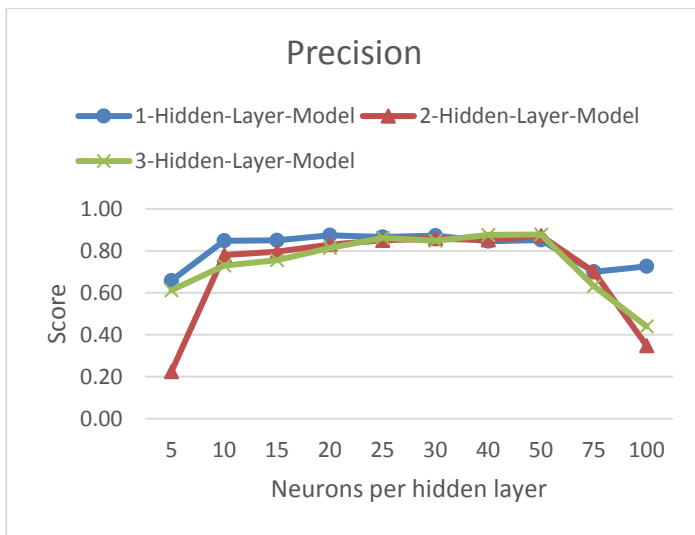


Figure 15: Precision of tested multi layer perceptron

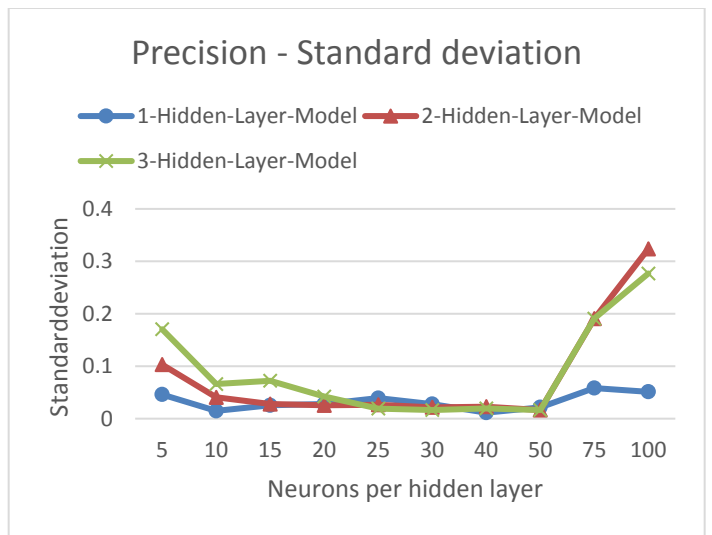


Figure 16: Precision - Standard deviation

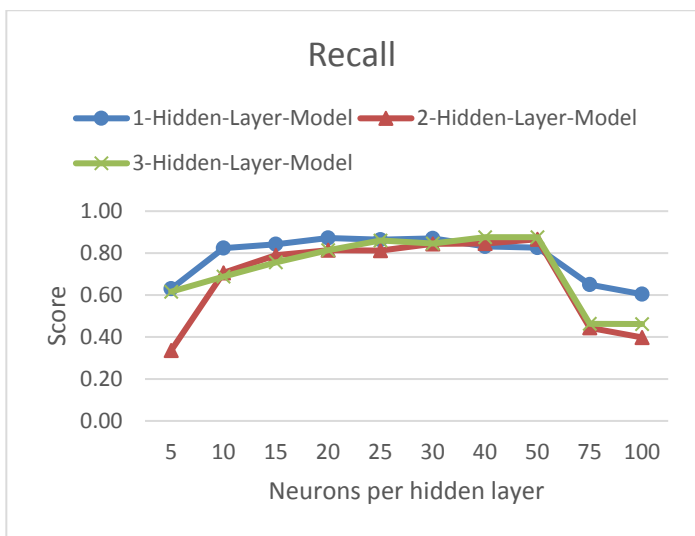


Figure 17: Recall of multi layer perceptron

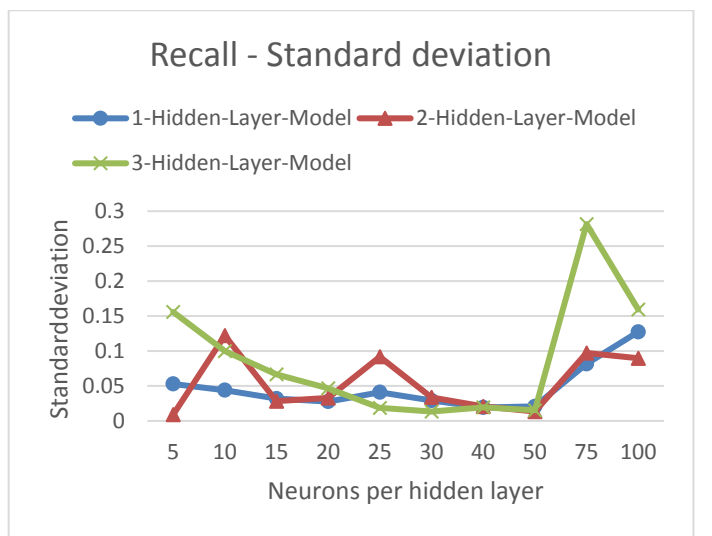


Figure 18: Recall - Standard deviation

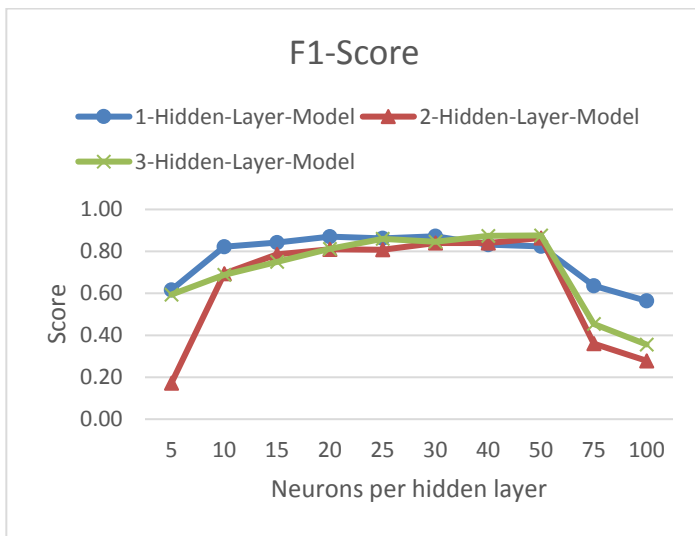


Figure 19: F1-Score of multi layer perceptron

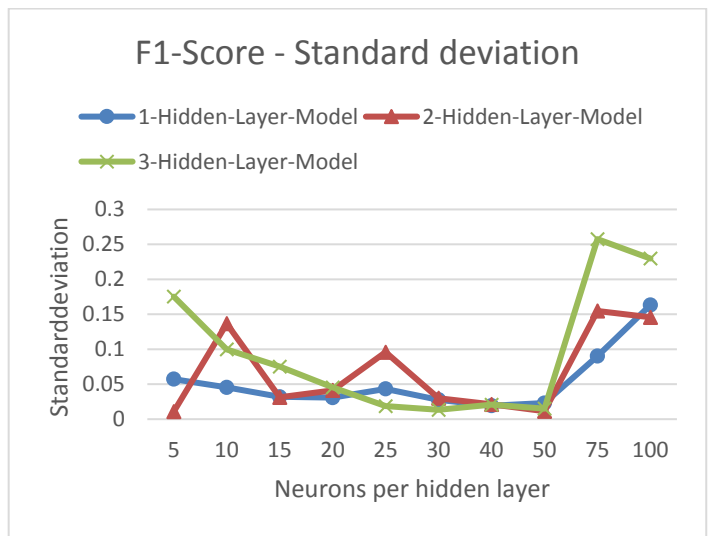


Figure 20: F1-Score - Standard deviation

After checking repeatability for a fixed dataset, five times cross validation with an 80/20 split (the dataset is split into five batches and all iterations of four training batches and one test batch are used to train and validate the ANN) is used to validate the model over the complete data set. The results of the cross validation are shown

in Table 5. The selected topology does not have quite as strong an effect through complete cross-validation. The achievable classification rates between 80 and 90 percent represent a good level for a first approach (no tweaking regarding learning rate, momentum etc. was done).

Model (neurons in one hidden layer)	Precision		Recall		F1-Score	
	Mean	Standard deviation	Mean	Standard deviation	Mean	Standard deviation
20	0.85	0.026	0.83	0.031	0.83	0.031
30	0.86	0.024	0.86	0.025	0.86	0.025
40	0.87	0.027	0.87	0.027	0.87	0.027
50	0.87	0.038	0.87	0.041	0.87	0.038

Table 5: Results of a fivefold cross-validation

A major drawback when working with such big datasets is computation performance. Training duration rises linear with the number of neurons in a hidden layer until a certain point, where it starts rising exponentially (Figure 21). This is probably due to the internal memory of the computer maxing out, so the operating system starts to cache data on the system disk. This process greatly reduces the speed of the training. Hence it is very important to have enough internal memory to not slow down the process. Furthermore, the batch size should not be too small. The overhead from various function calls increase the training time as well (Figure 22). Last, the final model will be stored on disk. Using a single hidden layer with a hundred neurons, the final model reaches almost 20 gigabytes (Figure 23). For further use, the model is loaded in memory, which decreases the available memory for batches or limits the maximum number neurons trainable.

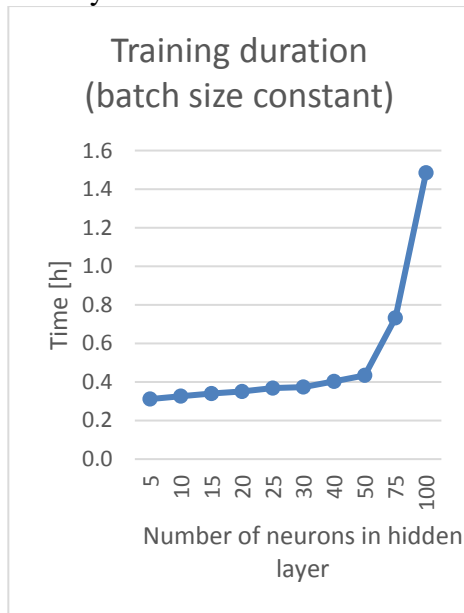


Figure 21: Training duration changes over hidden layer size

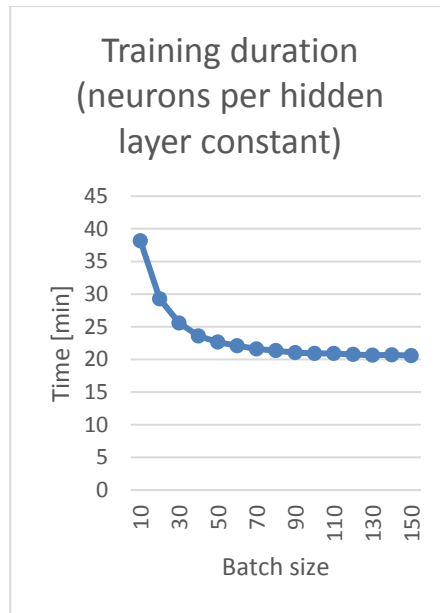


Figure 22: Training duration decreases with increasing batch size

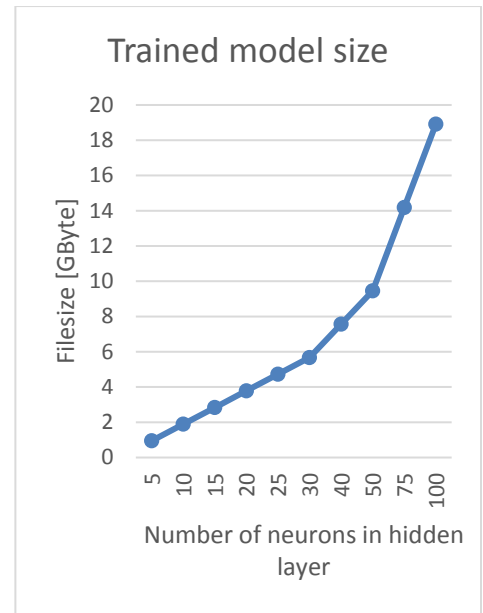


Figure 23: Final models get bigger with increasing complexity

Regarding the current classification the following statements can be made:

- Bottleneck approach is very useful, since roughly 12 million input neurons are used
- Three hidden-layer-topology offers best classification result, but also needs more computational resources
- Optimum between 25 and 45 neurons in hidden layer (also valid for multi-hidden-layer topologies)
- Maximum precision with this approach: 0.93
- Maximum recall with this approach: 0.93
- Maximum F1-score with this approach: 0.93
- ADAM is slower than SGD

These findings give a first impression how the artificial neural networks can be suitably designed to evaluate the acoustic signals of the process for an in-situ process monitoring.

6 Summary and Outlook

To detect pores in additive manufactured parts, a possible solution lies within an in-situ process monitoring. As a measurement technique, an acoustic sensor was chosen and implemented. The acquired process signals could be processed and were fed into an artificial neural network. It was possible to make a classification regarding the used laser power in the process. Multiple topologies of the artificial neural network were tested. A bottleneck approach with a single hidden layer seems the most promising. It can be concluded, that the acoustic signal of the process is suited to characterize the SLM process.

Once the final DOE is finished (all plates are printed), a bigger dataset will be created, and the different models will be tested against varying output classes. Using *Google TensorFlow* might decrease the overall time needed for training and testing. Furthermore, different parameter sets must be tested as well as other types of neural networks like convolutional neural networks or restricted Boltzmann machines.

After getting reference measures of the defects in the parts, it will be tried to correlate the defect type and position to the acoustic signals. The AI approach can easily be supplemented with additional input and output parameters to enable modular traceability. With this approach it should be possible to monitor the process and give a quantitative feedback on the estimated density or type of pores.

Acknowledgements

The research project „KitkAdd - Kombination und Integration etablierter Technologien mit additiven Fertigungsverfahren in einer Prozesskette“ (“Combination and integration of established technologies with additive manufacturing in one process chain”) is funded by the Bundesministerium für Bildung und Forschung (BMBF) in the program “Innovation für die Produktion, Dienstleistung und Arbeit von morgen” (02P15B017/02P15B015”) and supported by Projektträger Karlsruhe (PTKA). The authors are responsible for the content of this publication. We extend our gratitude to the BMBF for funding this research project and to all participants of “KitkAdd” for their collaboration and support.

7 References

- BDG (2010), *Volumendefizite von Gussstücken aus Aluminium-, Magnesium- und Zinkgusslegierungen*, P202.
- Berumen, S.; Bechmann, F.; Lindner, S.; Kruth, J.-P. & Craeghs, T. (2010), 'Quality control of laser- and powder bed-based Additive Manufacturing (AM) technologies', *Physics Procedia*, vol. 5, pp. 617–622.
- Calta, N. P.; Wang, J.; Kiss, A. M.; Martin, A. A.; Depond, P. J.; Guss, G. M.; Thampy, V.; Fong, A. Y.; Weker, J. N.; Stone, K. H.; Tassone, C. J.; Kramer, M. J.; Toney, M. F.; van Buuren, A. & Matthews, M. J. (2018), 'An instrument for in situ time-resolved X-ray imaging and diffraction of laser powder bed fusion additive manufacturing processes', *The Review of scientific instruments*, vol. 89, no. 5, p. 55101.
- Cherry, J. A.; Davies, H. M.; Mehmood, S.; Lavery, N. P.; Brown, S. G. R. & Sienz, J. (2015), 'Investigation into the effect of process parameters on microstructural and physical properties of 316L stainless steel parts by selective laser melting', *The International Journal of Advanced Manufacturing Technology*, vol. 76, no. 5, pp. 869–879.
- Clijsters, S.; Craeghs, T.; Buls, S.; Kempen, K. & Kruth, J.-P. (2014), 'In situ quality control of the selective laser melting process using a high-speed, real-time melt pool monitoring system', *The International Journal of Advanced Manufacturing Technology*, vol. 75, 5-8, pp. 1089–1101.
- Doubenskaia, M.; Pavlov, M. & Chivel, Y. (2010), 'Optical System for On-Line Monitoring and Temperature Control in Selective Laser Melting Technology', *Key Engineering Materials*, vol. 437, pp. 458–461.
- Eschner, N.; Lingenhöhl, J.; Öppling, S. & Lanza, G. (2017), 'Prozessüberwachung beim Laser Strahlschmelzen mit akustischen Signalen. Ein Vergleich verschiedener Sensorkonzepte und Integrationsmöglichkeiten', *wt Werkstattstechnik online 11/12 2017*, pp. 818–823.
- Everton, S. K.; Hirsch, M.; Stravroulakis, P.; Leach, R. K. & Clare, A. T. (2016), 'Review of in-situ process monitoring and in-situ metrology for metal additive manufacturing', *Materials & Design*, vol. 95, pp. 431–445.
- Furumoto, T.; Ueda, T.; Alkahari, M. R. & Hosokawa, A. (2013), 'Investigation of laser consolidation process for metal powder by two-color pyrometer and high-speed video camera', *CIRP Annals*, vol. 62, no. 1, pp. 223–226.
- García-Martín, J.; Gómez-Gil, J. & Vázquez-Sánchez, E. (2011), 'Non-destructive techniques based on eddy current testing', *Sensors (Basel, Switzerland)*, vol. 11, no. 3, pp. 2525–2565.
- Gebhardt, A. (2016), *Generative Fertigungsverfahren. Additive Manufacturing und 3D-Drucken für Prototyping - Tooling - Produktion*, Hanser, München. ISBN: 978-3446444010.
- Gevatter, H.-J. & Grünhaupt, U. (eds.) (2006), *Handbuch der Mess- und Automatisierungstechnik in der Produktion*, Springer-Verlag Berlin Heidelberg, Berlin, Heidelberg. ISBN: 978-3-540-34823-8.
- Gong, H.; Rafi, K.; Gu, H.; Starr, T. & Stucker, B. (2014), 'Analysis of defect generation in Ti–6Al–4V parts made using powder bed fusion additive manufacturing processes', *Additive Manufacturing*, 1-4, pp. 87–98.
- Grasso, M. & Colosimo, B. M. (2017), 'Process defects and in situ monitoring methods in metal powder bed fusion: a review', *Measurement Science and Technology*, vol. 28, no. 4, p. 44005.
- Haeckel, F. (2017), 'Technologische Herausforderungen für die automobilen Serienfertigung im Laserstrahlschmelzen' in *Rapid.Tech – International Trade Show & Conference for Additive Manufacturing*, eds M. Kynast, M. Eichmann & G. Witt, Carl Hanser Verlag GmbH & Co. KG, München, pp. 433–446. ISBN: 978-3-446-45459-0.
- Hirsch, M.; Catchpole-Smith, S.; Patel, R.; Marrow, P.; Li, W.; Tuck, C.; Sharples, S. D. & Clare, A. T. (2017), 'Meso-scale defect evaluation of selective laser melting using spatially resolved acoustic spectroscopy', *Proceedings. Mathematical, physical, and engineering sciences*, vol. 473, no. 2205, p. 20170194.
- Islam, M.; Purtonen, T.; Piili, H.; Salminen, A. & Nyrhilä, O. (2013), 'Temperature Profile and Imaging Analysis of Laser Additive Manufacturing of Stainless Steel', *Physics Procedia*, vol. 41, pp. 835–842.

- Kanko, J. A.; Sibley, A. P. & Fraser, J. M. (2016), 'In situ morphology-based defect detection of selective laser melting through inline coherent imaging', *Journal of Materials Processing Technology*, vol. 231, pp. 488–500.
- Khairallah, S. A.; Anderson, A. T.; Rubenchik, A. & King, W. E. (2016), 'Laser powder-bed fusion additive manufacturing. Physics of complex melt flow and formation mechanisms of pores, spatter, and denudation zones', *Acta Materialia*, vol. 108, pp. 36–45.
- Kief, H. B.; Roschiwal, H. A. & Schwarz, K. (2015), *CNC-Handbuch 2015/2016. CNC, DNC, CAD, CAM, FFS, SPS, RPD, LAN, CNC-Maschinen, CNC-Roboter, Antriebe, Energieeffizienz, Werkzeuge, Industrie 4.0, Fertigungstechnik, Richtlinien, Normen, Simulation, Fachwortverzeichnis*, Hanser, München. ISBN: 3446440909.
- Kiefel, D.; Scius-Bertrand, M. & Stöbel, R. (2018), 'Computed Tomography of Additive Manufactured Components in Aeronautic Industry', *8th Conference on Industrial Computed Tomography*, vol. 2018.
- Krauss, H. (2016), *Qualitätssicherung beim Laserstrahlschmelzen durch schichtweise thermografische In-Process-Überwachung*. Dissertation, Herbert Utz Verlag GmbH.
- Krauss, H.; Eschey, C. & Zaeh, M. F. (2012), 'Thermography for monitoring the selective laser melting process', *Proceedings of the Solid Freeform Fabrication Symposium*, vol. 2012, pp. 999–1014.
- Lanza, G.; Kopf, R.; Zaiß, M.; Stricker, N.; Eschner, N.; Jacob, A.; Yang, S.; Schönle, A.; Webersinke, L. & Wirsig, L. (2017), *Laser-Strahlschmelzen - Technologie mit Zukunftspotenzial. Ein Handlungsleitfaden*, KIT - Karlsruhe Institut für Technologie, wbk Institut für Produktionstechnik, Karlsruhe. ISBN: 978-3-00-056913-5.
- Leuders, S.; Thöne, M.; Riemer, A.; Niendorf, T.; Tröster, T.; Richard, H. A. & Maier, H. J. (2013), 'On the mechanical behaviour of titanium alloy TiAl6V4 manufactured by selective laser melting. Fatigue resistance and crack growth performance', *International Journal of Fatigue*, vol. 48, pp. 300–307.
- Liu, Y. J.; Li, S. J.; Wang, H. L.; Hou, W. T.; Hao, Y. L.; Yang, R.; Sercombe, T. B. & Zhang, L. C. (2016), 'Microstructure, defects and mechanical behavior of beta-type titanium porous structures manufactured by electron beam melting and selective laser melting', *Acta Materialia*, vol. 113, pp. 56–67.
- Lott, P.; Schleifenbaum, H.; Meiners, W.; Wissenbach, K.; Hinke, C. & Bültmann, J. (2011), 'Design of an Optical system for the In Situ Process Monitoring of Selective Laser Melting (SLM)', *Physics Procedia*, vol. 12, pp. 683–690.
- Ly, S.; Rubenchik, A. M.; Khairallah, S. A.; Guss, G. & Matthews, M. J. (2017), 'Metal vapor micro-jet controls material redistribution in laser powder bed fusion additive manufacturing', *Scientific Reports*, vol. 7, no. 1, p. 127.
- Neef, A.; Seyda, V.; Herzog, D.; Emmelmann, C.; Schönleber, M. & Kogel-Hollacher, M. (2014), 'Low Coherence Interferometry in Selective Laser Melting', *Physics Procedia*, vol. 56, pp. 82–89.
- Purtonen, T.; Kalliosaari, A. & Salminen, A. (2014), 'Monitoring and Adaptive Control of Laser Processes', *Physics Procedia*, vol. 56, pp. 1218–1231.
- Reschetnik, W. (2017), *Lebensdauerorientierte Eigenschaftsänderungen von additiv gefertigten Bauteilen und Strukturen*. Dissertation, Universität Paderborn, Paderborn.
- Rieder, H.; Spies, M.; Bamberg, J. & Henkel, B. (2016), 'On- and offline ultrasonic characterization of components built by SLM additive manufacturing'. *42nd annual review of progress in quantitative nondestructive evaluation: Incorporating the 6th European-American Workshop on Reliability of NDE*, AIP Publishing LLC, p. 130002.
- Schild, L.; Kraemer, A.; Reiling, D.; Wu, H. & Lanza, G. (2018), 'Influence of surface roughness on measurement uncertainty in Computed Tomography', *8th Conference on Industrial Computed Tomography, Wels, Austria (iCT 2018)*.
- Shedlock, D.; Edwards, T. & Toh, C. (2011), 'X-ray backscatter imaging for aerospace applications.'. *AIP Conference Proceedings*, AIP, pp. 509–516.

- Shevchik, S. A.; Kenel, C.; Leinenbach, C. & Wasmer, K. (2018), 'Acoustic emission for in situ quality monitoring in additive manufacturing using spectral convolutional neural networks', *Additive Manufacturing*, vol. 21, pp. 598–604.
- Smith, R. J.; Hirsch, M.; Patel, R.; Li, W.; Clare, A. T. & Sharples, S. D. (2016), 'Spatially resolved acoustic spectroscopy for selective laser melting', *Journal of Materials Processing Technology*, vol. 236, pp. 93–102.
- Spears, T. G. & Gold, S. A. (2016), 'In-process sensing in selective laser melting (SLM) additive manufacturing', *Integrating Materials and Manufacturing Innovation*, vol. 5, no. 1, p. 683.
- Spierings, A. B.; Schneider, M. & Eggenberger, R. (2011), 'Comparison of density measurement techniques for additive manufactured metallic parts', *Rapid Prototyping Journal*, vol. 17, no. 5, pp. 380–386.
- Thijs, L.; Verhaeghe, F.; Craeghs, T.; van Humbeeck, J. & Kruth, J.-P. (2010), 'A study of the microstructural evolution during selective laser melting of Ti–6Al–4V', *Acta Materialia*, vol. 58, no. 9, pp. 3303–3312.
- Toepfel, T.; Schumann, P.; Ebert, M.-C.; Bokkes, T.; Funke, K.; Werner, M.; Zeulner, F.; Bechmann, F. & Herzog, F. (2016), '3D analysis in laser beam melting based on real-time process monitoring'. *Mater Sci Technol Conf*, pp. 123–132.
- van Elsen, M. (2007), *Complexity of Selective Laser Melting: a new optimisation approach*. Dissertation, KU Leuven, Leuven, Faculteit Ingenieurswetenschappen.
- Yadollahi, A. & Shamsaei, N. (2017), 'Additive manufacturing of fatigue resistant materials. Challenges and opportunities', *International Journal of Fatigue*, vol. 98, pp. 14–31.
- Ye, D.; Hong, G. S.; Zhang, Y.; Zhu, K. & Fuh, J. Y. H. (2018), 'Defect detection in selective laser melting technology by acoustic signals with deep belief networks', *The International Journal of Advanced Manufacturing Technology*, vol. 593, no. 1, p. 170.
- Zenzinger, G.; Bamberg, J.; Henkel, B.; Hess, T. & Ladewig, A. (2014), 'Online-Prozesskontrolle bei der additiven Fertigung mittels Laserstrahlschmelzen', *DGZfP Zeitung*, no. 140, pp. 51–54.
- Zur Jacobsmühlen, J.; Kleszczynski, S.; Witt, G. & Merhof, D. (2015), 'Elevated region area measurement for quantitative analysis of laser beam melting process stability'. *26th International Solid Freeform Fabrication Symposium; Austin, TX*, pp. 549–559.